

PAPER • OPEN ACCESS

Charge transfer mechanisms in multistructured photoelectrodes for perovskite solar cells

To cite this article: M F Vildanova *et al* 2020 *J. Phys.: Conf. Ser.* **1697** 012187

View the [article online](#) for updates and enhancements.

You may also like

- [Recent progress in efficient hybrid lead halide perovskite solar cells](#)
Jin Cui, Huaaliang Yuan, Junpeng Li *et al.*
- [Layered perovskite materials: key solutions for highly efficient and stable perovskite solar cells](#)
Chintam Hanmandlu, Anupriya Singh, Karunakara Moorthy Boopathi *et al.*
- [Physics of defects in metal halide perovskites](#)
Chunxiong Bao and Feng Gao



ECS
The
Electrochemical
Society
Advancing solid state &
electrochemical science & technology

DISCOVER
how sustainability
intersects with
electrochemistry & solid
state science research

Charge transfer mechanisms in multistructured photoelectrodes for perovskite solar cells

M F Vildanova, A B Nikolskaia, S S Kozlov and O I Shevaleevskiy

Solar Photovoltaic Department, Institute of Biochemical Physics, Russian Academy of Sciences, Kosygin St. 4, Moscow, 119334, Russia

mvildanova@sky.chph.ras.ru

Abstract. Here we introduce the research studies of perovskite solar cells with multistructured photoelectrodes based on very wide bandgap nanocrystalline materials. A series of solar cells with the device architecture FTO/c-TiO₂/ZrO₂(HfO₂)/CH₃NH₃PbI₃/Spiro-MeO-TAD/Au was fabricated and characterized. The results obtained demonstrate a successful possibility of PV application of the nanostructured oxide materials with bandgap values exceeding 5 eV. We propose a mechanism, which describes charge carrier transport at the interface of perovskite/multistructured photoelectrode.

1. Introduction

Nanostructured materials are widely used in next generation photovoltaic devices including organic-inorganic metal halide perovskite solar cells (PSCs), which are suitable for mass production technologies. A key component of the PSC is a thin film nanostructured photoelectrode, which in general based on titanium dioxide (TiO₂) with a band gap (E_g) of 3.0-3.2 eV. The applicability of photoelectrodes based on very wide bandgap materials with $E_g > 5$ eV has always been controversial, because the charge carrier transport deteriorates with the increase of E_g . However, very wide bandgap nanostructured systems were shown to be efficient for solar cell application [1-2].

Several configurations for PSCs have been reported in literature. One of them includes very wide bandgap mesoporous scaffold. The pioneer study reported by the group of H. Snaith introduces Al₂O₃ scaffold, replacing traditional TiO₂ electron transport layer [3]. Later PV application of different insulating materials was investigated, including zirconia (ZrO₂) nanostructured films with $E_g \sim 5.6$ eV [4]. Recently, we have studied charge transfer kinetics in ZrO₂-based PSCs and showed that such materials could be successfully used as photoelectrodes in PSCs [5].

Yet another cell architecture represents a multiple layered electron transport system, including thin TiO₂ and ZrO₂ layers [6]. Incorporation of an additional thin layer of a wide bandgap oxide in the mesoporous structure is reported to be advantageous. It was shown that large dielectric constant of ZrO₂ removes Coulomb attraction between charge carriers and facilitates ambipolar transport by effective charge screening [7]. The both mentioned above solutions demonstrate improvement in the PV performance of PSCs compared to the state-of-the-art TiO₂ mesoporous layers (m-TiO₂).

In the frames of this study we also introduce hafnium dioxide (HfO₂)-based nanostructures with E_g exceeding 5.6 eV, which present interest for fabrication of efficient photoelectrodes for PSCs. Among the metal oxides from groups IV and V HfO₂ attracts considerable attention, adopting the similar structure with ZrO₂. Thus, we prepared and investigated ZrO₂- and HfO₂-based nanostructured thin



films, which were used for fabrication of the multistructured photoelectrodes for PSCs with the device architecture of glass/FTO/c-TiO₂/MO₂/CH₃NH₃PbI₃/Spiro-MeO-TAD/Au (where M = Zr, Hf; c-TiO₂ is ~20 nm TiO₂ compact layer).

2. Experimental

2.1. Fabrication of PSCs with multistructured nanocrystalline photoelectrodes

Two series of PSCs with multilayered structures and the device architecture denoted as FTO/c-TiO₂/MO₂/CH₃NH₃PbI₃/Spiro-MeO-TAD/Au (where M = Zr, Hf) were fabricated. The fabrication of PSCs was carried out under ambient conditions (RH ~50%), following the previously developed technology [8]. ZrO₂ and HfO₂ nanoparticles were obtained by hydrothermal treatment of co-precipitated zirconium and hafnium hydroxides from solutions of the corresponding metal salts [5]. Thick pastes from MO₂ nanopowders were prepared in organic solvent following the method suitable for TiO₂ [9]. The pastes were dissolved in ethanol in mass ratio 1:5 and spin-coated onto thin c-TiO₂ layer with subsequent annealing at 500°C for 30 min. Perovskite layer CH₃NH₃PbI₃ was formed on MO₂ using a conventional one-step deposition method [10].

2.2. Characterization of multistructured layers and PSCs

Film morphology of the multistructured photoelectrodes was investigated using a dual-beam scanning electron microscope (SEM) Helios NanoLab 660 (FEI, USA). The topography of the photoelectrode surface was measured via atomic force microscopy (AFM) using a scanning probe microscope NTEGRA Prima (NT-MDT, Russia). Absorption characteristics were calculated from diffuse reflectance spectra of MO₂ nanopowders recorded using Shimadzu UV-3600 spectrophotometer (Shimadzu, Japan) with an ISR-3100 integrating sphere in the wavelength range of 300-1200 nm. The current density-voltage (*J-V*) curves were measured using the SCS-4200 Semiconductor Characterization System (Keithley, USA) under standard AM1.5G illumination conditions (1000 W/m²) using Abet 10500 Solar Simulator (Abet Technologies, USA). The incident photon-to-current conversion efficiency (IPCE) spectra were recorded using QEX10 Solar Cell Quantum Efficiency Measurement System (PV Measurements, USA) in the range of 300-900 nm.

3. Results and Discussion

3.1. UV-vis absorption spectroscopy

Figure 1 shows a function of optical absorption coefficient (α) for MO₂ nanopowders. As the nanopowders are highly light scattering materials, their absorption characteristics were calculated from the diffuse reflectance spectra applying Kubelka-Munk theory [11].

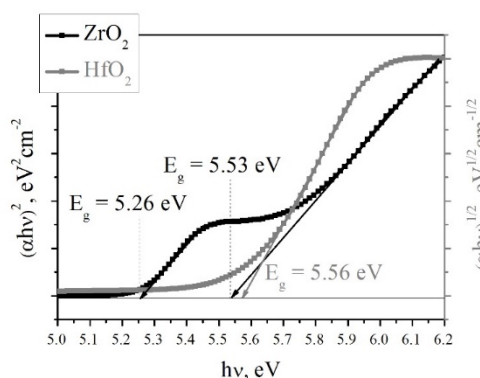


Figure 1. $(\alpha hv)^n$ vs. photon energy for ZrO₂ and HfO₂ nanopowders and their bandgap values calculated.

The E_g values for MO₂ were estimated according to Tauc's law [12] by extrapolation of the linear segments of $(\alpha hv)^n$ plot (where $n = 2$ for direct and $n = 1/2$ for indirect bandgap) to the photon energy

axis. Monoclinic modification of ZrO_2 was found to have two direct band transitions [5] with the values of 5.26 and 5.53 eV. HfO_2 absorption region fits to the characteristics of an indirect bandgap [13] with the value of 5.56 eV.

3.2. Scanning electron microscopy (SEM)

Surface morphologies of multistructured photoelectrodes, consisting of thin c- TiO_2 layer coated with MO_2 mesoporous layers were studied by means of SEM.

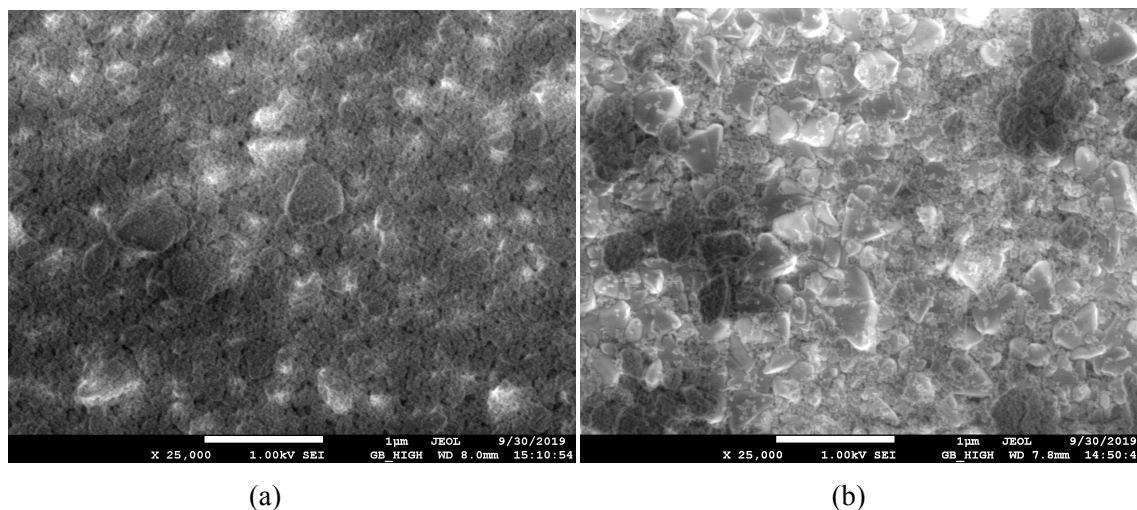


Figure 2. Surface SEM images of ZrO_2 (a) and HfO_2 (b) layers deposited onto c- TiO_2 layer.

Figure 2a shows SEM image of the ZrO_2 thin layer deposited on c- TiO_2 layer. The agglomeration of sphere-like crystallites is observed. The average particle size ranges from 30 to 40 nm. The layer surface looks to be irregular. Such a suitable surface morphology is essential for high PV performance, compared to planar PSCs containing single c- TiO_2 . In this case ZrO_2 eliminates pinholes, normally occurring in thin c- TiO_2 layers. As a result, it plays a role of a blocking layer, which avoids the undesired charge transport to the contact. Moreover, the observed agglomeration of ZrO_2 nanoparticles leads to better light scattering, thus increasing the charge carrier diffuse length.

HfO_2 was found to show similar surface morphology (see Figure 2b). However, the layer is even less uniform, compared to ZrO_2 . The average particle size in HfO_2 layer is about 30 nm. Nanoparticles demonstrate less agglomeration and the distribution is more dispersed with weaker interparticle necking.

3.3. Atomic force microscopy (AFM)

Surface configuration of multistructured photoelectrodes was studied by means of AFM. Figure 3 shows the current mapping in the mesoporous TiO_2 (a), ZrO_2 (b) and HfO_2 (c) layers deposited onto c- TiO_2 /FTO.

FTO has large grains, so the layer has high surface roughness. It shows high conductivity with electrical current values reaching 30 nA under 4 V bias. c- TiO_2 layer is extremely thin, so it doesn't smooth the surface roughness. Its conductivity is reasonably lower, compared to FTO. However, due to pinholes in the layer there are some regions with higher current flow (up to 25 nA). Regular mesoporous TiO_2 layer, which is used as a photoelectrode in the state-of-the-art PSCs (Figure 3a) has low conductivity, but it shows a uniform distribution over the surface. The highest current value is 350 pA.

On the contrary, ZrO_2 nanoparticles form an irregular layer, as shown in Figure 2a. Deposited on the surface with high roughness, it fills the cavities, leaving some areas of the surface uncovered. Thus, in Figure 3b we see the local regions with the increased current (red spots with the values up to

25 nA), associated with c-TiO₂ uncovered with ZrO₂. Despite the insulating nature of ZrO₂, the highest current flow was obtained through the multistructured c-TiO₂/ZrO₂ layer.

As for HfO₂ (Figure 3c), it demonstrates similar behavior with ZrO₂. Due to the specific distribution of the particles over the surface, its conductive regions are spread more dispersed with lower current flow, not exceeding 18 nA.

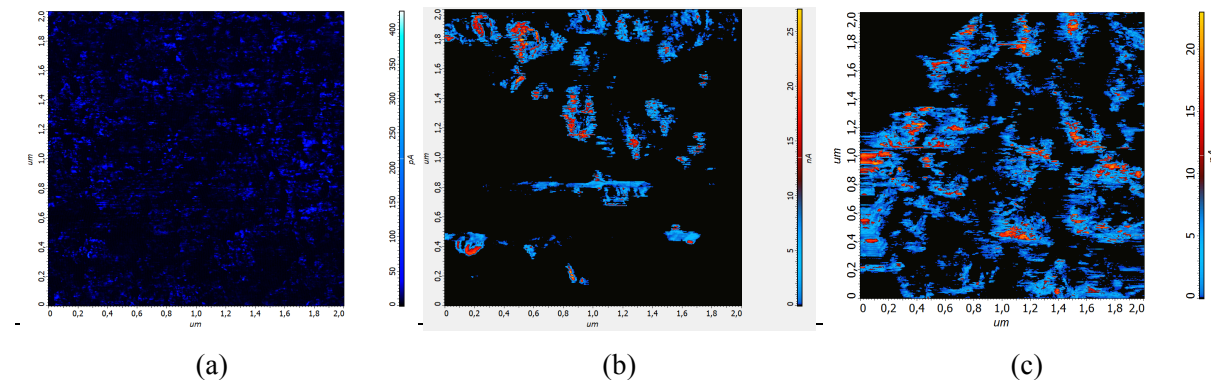


Figure 3. AFM micrographs of the current mapping in TiO₂ (a) ZrO₂ (b) and HfO₂ (c) layers deposited onto c-TiO₂/FTO.

3.4. Photovoltaic properties

The *J-V* curves and IPCE spectra of the fabricated devices with the architecture of glass/FTO/c-TiO₂/MO₂/CH₃NH₃PbI₃/Spiro-MeO-TAD/Au are shown in Figure 4. Photovoltaic parameters of the solar cells are listed in Table 1.

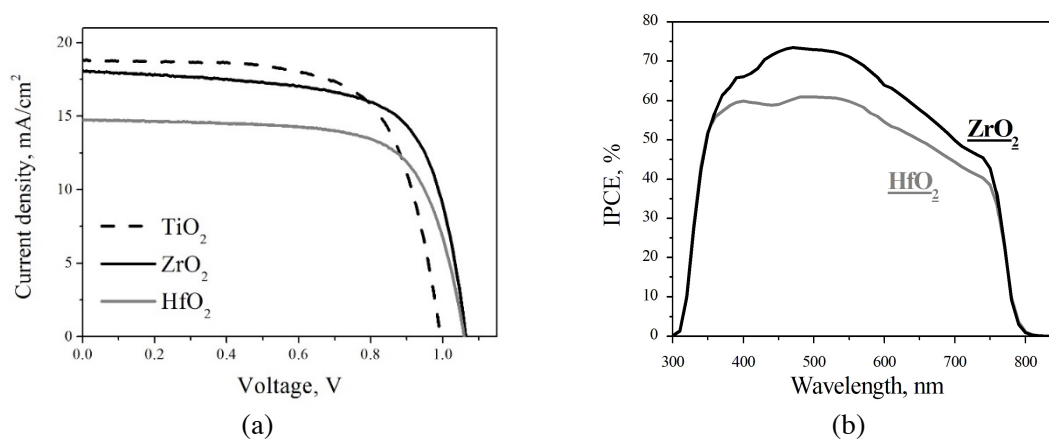


Figure 4. *J-V* curves (a) and IPCE spectra (b) for the champion PSC devices based on multistructured ZrO₂, HfO₂ photoelectrodes and conventional mesoporous TiO₂ photoelectrodes.

State-of-the-art devices with bare TiO₂ photoelectrodes show the average power conversion efficiency (PCE) of 12.64% with short circuit current density (J_{SC}), open circuit voltage (V_{OC}) and fill factor (FF) reaching 19.05 mA/cm², 0.99 V and 0.67, respectively. With the substitution of m-TiO₂ layer with a wide bandgap mesoporous structure MO₂ we observe the improvement of PV performance, compared to state-of-the-art devices. The major difference is in the V_{OC} values, which is attributed to the difference in the conduction band (CB) positions of TiO₂ and MO₂. However, with incorporation of the wide bandgap materials a slight drop in J_{SC} is found, which can be explained by the insulating nature of MO₂. According to the band structure, there should be no charge separation

between $\text{MO}_2/\text{CH}_3\text{NH}_3\text{PbI}_3$. Thus, the electrons are accumulated at the interface with the following transport via c-TiO_2 , being in the direct contact with perovskite, while MO_2 layer is deposited irregularly on the surface.

The highest device performance was shown by the PSCs with $\text{c-TiO}_2/\text{ZrO}_2$ electron transporting layers. An average PCE is 13.30%, J_{SC} , V_{OC} and FF are 17.96 mA/cm^2 , 1.06 V and 0.70, respectively. PV parameters increased up to 10% with the use of multistructured photoelectrodes, while the champion device's efficiency reached 14.02% compared to 12.81% for state-of-the-art one. HfO_2 -based PSCs show poorer PV performance (up to 10.97%) due to lower J_{SC} values. In this case ZrO_2 may be more advantageous in the way of its light scattering properties. As the IPCE is related to J_{SC} , the higher values of ZrO_2 -based PSCs, compared to HfO_2 -based ones (see Figure 4b), correspond to the improved J_{SC} .

Table 1. PV parameters of PSCs with conventional mesoporous TiO_2 photoelectrodes and multistructured photoelectrodes based on ZrO_2 and HfO_2 .

	J_{SC} , mA/cm^2	V_{OC} , V	FF , a.u.	PCE, %
TiO_2	19.05 ± 0.17	0.99 ± 0.007	0.67 ± 0.01	12.64 ± 0.26
ZrO_2	17.96 ± 0.28	1.06 ± 0.008	0.70 ± 0.04	13.30 ± 0.99
HfO_2	14.25 ± 0.92	1.06 ± 0.003	0.70 ± 0.02	10.49 ± 0.96

3.5. Charge transfer mechanism

The major difference between the cells energy band structure (see Figure 5) compared to the state-of-the-art PSCs concerns the different charge transport mechanisms at the perovskite/photoelectrode interface for MO_2 and TiO_2 electrodes.

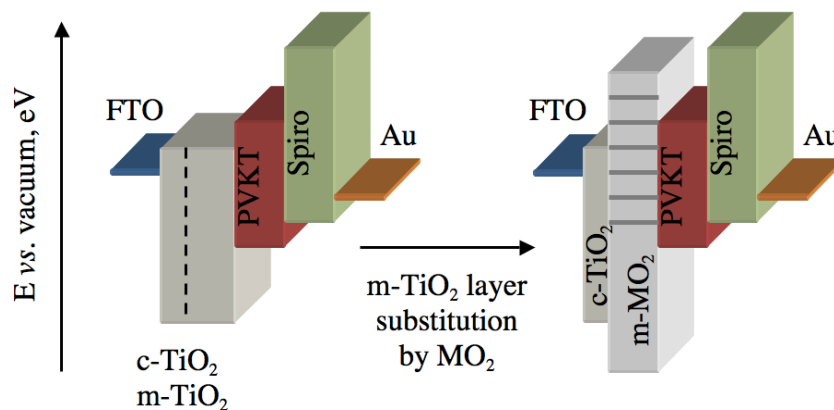


Figure 5. Architectures of the PSCs with multistructured photoelectrodes with their band energy diagram, compared to the state-of-the-art TiO_2 -based PSCs. Here $M = \text{Zr, Hf}$.

The CB edge of both ZrO_2 and HfO_2 is located much higher on the energy diagram, compared to the CB edge of perovskite, which makes the electron transfer from perovskite to the photoelectrode impossible in terms of the classical charge transfer mechanism. On the other hand, electron hopping through the states localized within the bandgap as a proposed charge transfer mechanism was discussed in our previous work [14]. However, it has a minor impact on the total charge transport in the photoelectrodes. Electron transport through CB of c-TiO_2 is a dominating process. Its efficiency is

increased due to insertion of the wide bandgap material, which acts both as a scaffold and charge collection layer at the interface with ambipolar perovskite.

Poorer PV performance observed in HfO₂-based PSCs in comparison with ZrO₂-based devices is more likely attributed to the insufficient layer morphology and less favorable positions of the electronic states in HfO₂ forbidden zone.

4. Conclusions

In this paper we have demonstrated that very wide bandgap nanostructured oxide materials, like ZrO₂ and HfO₂, with E_g exceeding 5 eV, can be successfully used for PV application for constructing multistructured electron transporting photoelectrodes. These oxides were used for fabrication of PSCs with the device architecture of glass/FTO/c-TiO₂/MO₂/CH₃NH₃PbI₃/Spiro-MeO-TAD/Au (M = Zr, Hf). The incorporation of mesoporous MO₂ layer led to the improvement of PV performance up to 10%. The increase in the V_{OC} is explained by the difference in CB positions of TiO₂ and MO₂ and the light scattering properties of MO₂ in the multilayered system results in the sufficient J_{SC} . Despite the insulating nature of MO₂, very wide band-gap materials play an important role in the efficient electron transport in PSCs. Here we have proposed the mechanism, describing charge carrier transfer at the interface of perovskite/multistructured photoelectrode. It has been shown that an irregular layer of a very wide bandgap material formed on the c-TiO₂ surface acts both as a scaffold and charge collection layer at the interface, resulting in the improved PV performance.

Acknowledgements

This work was supported by the Russian Science Foundation under grant No. 20-69-47124.

References

- [1] Ranjitha S, LavanyaDhevi R, Hariharan V, Anbarasan P M, Priya R S and Sridharan M 2018 *Int. J. Adv. Sci. Eng.* **5**(2) 948
- [2] Ball J M, Lee M M, Hey A and Snaith H J 2013 *Energ. Environ. Sci.* **6**(6) 1739
- [3] Lee M M, Teuscher J, Miyasaka T, Murakami T N and Snaith H J 2012 *Science* **338** 634
- [4] Bi D, Moon S J, Häggman L, Boschloo G, Yang L, Johansson E M, Nazeeruddin M K, Grätzel M and Hagfeldt A 2013 *RSC Adv.* **3**(41) 18762
- [5] Larina L L, Alexeeva O V, Almjasheva O V, Gusarov V V, Kozlov S S, Nikolskaia A B, Vildanova M F and Shevaleevskiy O I 2019 *Nanosyst. Phys. Chem. Math.* **10**(1) 70
- [6] Mejia Escobar M A, Pathak S, Liu J, Snaith H J and Jaramillo F 2017 *ACS Appl. Mater. Interfaces* **9**(3) 2342
- [7] Juarez-Perez E J, Sanchez R S, Badia L, Garcia-Belmonte G, Kang Y S, Mora-Sero I and Bisquert J 2014 *J. Phys. Chem. Lett.* **5**(13) 2390
- [8] Shevaleevskiy O I, Nikolskaia A B, Vildanova M F, Kozlov S S, Alexeeva O V, Vishnev A A and Larina L L 2018 *Russ J. Phys. Chem. B* **12**(4) 663
- [9] Ito S, Chen P, Comte P, Nazeeruddin M K, Liska P, Péchy P and Grätzel M 2007 *Prog Photovoltaics: Res. Appl.* **15**(7) 603
- [10] Park N G 2016 *Nano Converg.* **3**(1) 15
- [11] Kubelka P 1948 *J. Opt. Soc. Am.* **38** 448
- [12] Tauc J, Grigorovici R and Vancu A 1966 *Phys. St. Sol.* **15** 627
- [13] Martínez F L, Toledano-Luque M, Gandía J J, Cárabe J, Bohne W, Röhrich J, Sturb E and Mártel I 2007 *J. Phys. D Appl. Phys.* **40**(17) 5256
- [14] Vildanova M F, Nikolskaia A B, Kozlov S S, Karyagina O K, Larina L L, Shevaleevskiy O I, Almjasheva O V and Gusarov V V 2019 *Dokl. Phys. Chem.* **484**(2) 36